Table S-1. The concentration of the gas being detected at different humidity levels.

Gas mixtures	RH=20%	RH=30%	RH=50%	RH=70%
	(5,1,5, 20%)	(5,1,5, 30%)	(5,1,5, 50%)	(5,1,5, 70%)
	(7,3,7, 20%)	(7,3,7, 30%)	(7,3,7,50%)	(7,3,7, 70%)
$NH_3, C_8H_{10}, HCHO$(ppm)	(9,5,9, 20%)	(9,5,9, 30%)	(9,5,9,50%)	(9,5,9, 70%)
	(11,7,11, 20%)	(11,7,11, 30%)	(11,7,11,50%)	(11,7,11, 70%)
	(13,9,13, 20%)	(13,9,13, 30%)	(13,9,13,50%)	(13,9,13, 70%)
	(15,11,15, 20%)	(15,11,15,30%)	(15,11,15,50%)	(15,11,15, 70%)

Table S-2. Comparison results of the difference between the actual concentration and the predicted concentration.

Actual value(ppm)	C_8H_{10} (ppm)		Actual value(ppm)	NH_3 (ppm)		$HCHO$ (ppm)	
	Predicted	Error value		Predicted	Error value	Predicted	Error value
1	0.8730	-0.1270	5	4.4279	-0.5721	4.8501	-0.1799
3	3.4970	0.4970	7	6.7070	-0.2930	6.7325	-0.2675
5	5.4451	0.4451	9	9.440	0.4405	8.5984	-0.4016
7	7.7452	0.7452	11	10.8530	-0.1470	11.3445	0.3455
9	9.1269	0.1269	13	13.1344	0.1344	12.9246	-0.1749
11	11.8338	0.8338	15	15.6328	0.5328	15.8294	0.8294

Table S-3. Comparative analysis of BPNN and SSA-BPNN performance parameters

Performance parameter	BPNN			SSA-BPNN		
	NH_3	C_8H_{10}	$HCHO$	NH_3	C_8H_{10}	$HCHO$
MAE	0.6109	0.6762	0.6455	**0.5567**	**0.6548**	**0.6137**
MAPE(%)	4.667	7.636	7.206	**3.2161**	**5.567**	**5.276**
MSE	0.5067	0.5466	0.5596	**0.4519**	**0.4846**	**0.4686**
RMSE	0.5116	0.5579	0.5496	**0.4785**	**0.5367**	**0.5267**

The key machine learning codes including the optimization codes

net=newff(inputn,outputn,hiddennum,{'tansig','purelin'},'trainlm');

%The framework of the SSA

Input:

G:the maximum ilerations

PD:the number of the producers

SD:the number of the sparrows who perccive the dangcr

R2:the alarm value

Establish an objective function F(X),wherc variable $X=(x_1, x_2, x_3,…, x_d)$.

Initalizea popuaton of N sparrows and define its relevant paramefers.

Output: Xbest ,fg.

l: while the maximum iterations G is not met do

2:     Rank the finess values and find the current bes individual and the current worst individual.

3:     R2 = rand(1)

4:     for i =1 : PD

5:     Using equation (3-4) update the sparrow's location;

6:     end for

7:     for i= (PD+1) : n

8:     Using equation (3-5) update the sparrow's locatio;

9:     end for

10:    for i= 1 : SD

11:    Using equation (3-6) update the sparrow's location;

12:    end for

13:    Get the current new location;

14:    If the new location is better than before,update it;

15:    t= t + 1

16:    end while

17:    return Xbest , fg.

x= Xbest

w1=x(1:inputnum*hiddennum);

B1=x(inputnum*hiddennum+1:inputnum*hiddennum+hiddennum);

w2=x(inputnum*hiddennum+hiddennum+1:inputnum*hiddennum+hiddennum+hiddennum*outputnum);

B2=x(inputnum*hiddennum+hiddennum+hiddennum*outputnum+1:inputnum*hiddennum+hiddennum+hiddennum*outputnum+outputnum);

net.iw{1,1}=reshape(w1,hiddennum,inputnum);

net.lw{2,1}=reshape(w2,outputnum,hiddennum);

net.b{1}=reshape(B1,hiddennum,1);

net.b{2}=reshape(B2,outputnum,1);

%Set initial parameters of BP network (training times, learning rate, minimum error of training target):

net.trainParam.epochs=1000;

net.trainParam.lr=0.1;
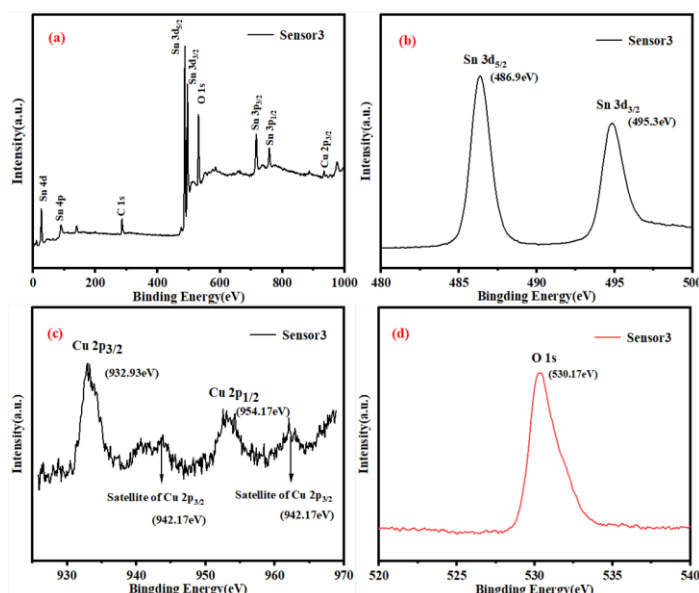
net.trainParam.goal=0.001;

Fig.S1 XPS spectra of (14wt%) Cu/SnO$_2$ nanomaterials:
(a) Cu/SnO$_2$; (b) Sn 3d; (c) Cu 2p; (d)O 1s

As shown in Fig.S1, the electronic state and binding energy of the grown heterojunction structure are measured by XPS technology. Fig.S1(a) shows the XPS peaks corresponding to the characteristics of Sn, Cu and O atoms. Fig.S1(b) shows the peaks with binding energies of 486.9eV and 495.3eV are consistent with the core energy spectrum of Sn 3d$_{5/2}$ and Sn 3d$_{3/2}$, confirming that metal Sn exists in SnO$_2$. Fig.S1(c) shows two peaks at 932.93 eV and 954.17 eV. They correspond to Cu 2p$_{3/2}$ and Cu 2p$_{1/2}$ states, which confirms that CuO contains Cu. The O 1s peak with binding energy of 530.1 eV is shown in Fig.S1(d), which confirms the existence of O in Cu/SnO$_2$ nanostructures.
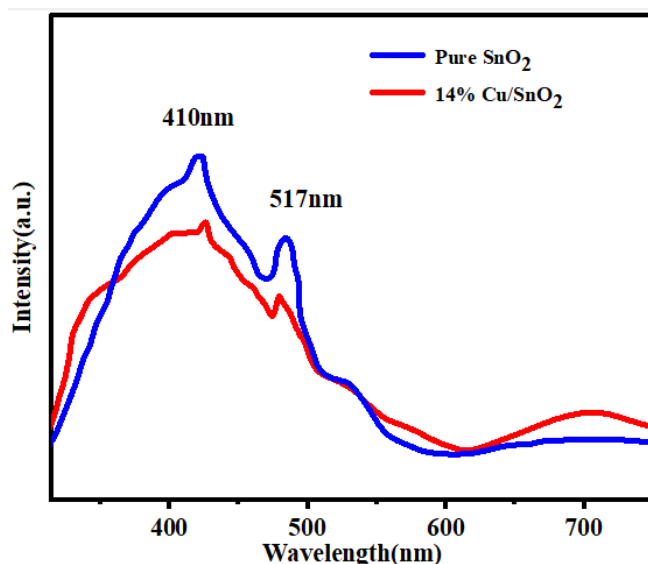

Fig.S2 Photoluminescence spectra of pure SnO$_2$ and (14wt%)
Cu/SnO$_2$ nanomaterials.

Fig.S2 shows the room temperature photoluminescence spectra of the synthesized pure SnO$_2$ and (14wt%) Cu/SnO$_2$ nanomaterials. In the two materials, there are two strong emissions

corresponding to 410 nm and 517 nm. Among them, V_O^0, V_O^+ and V_O^{++} are the most common defects, which are caused by oxygen vacancies and trapped electrons from the valence band, and may act as luminescent centers in the band gap. When the sample is exposed to ultraviolet radiation, the electrons are excited from the valence band to the conduction band, leaving a hole valence band in the sample. This active hole recombines with the electrons in the deep trap V_O^+ to form V_O^{++} center. When the conduction band electrons recombine with the V_O^{++} center, visible emission is generated.
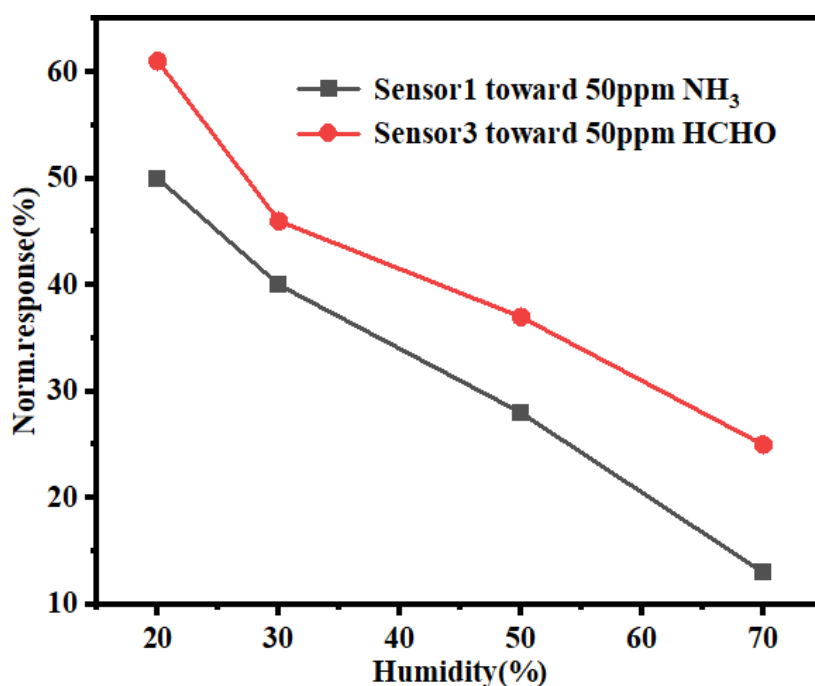

Fig.S3 Response curve of sensor with humidity

Fig.S3 shows the curves of the response of Sensor1 and Sensor3 to ammonia and formaldehyde, respectively, as the relative humidity increases. As can be seen from the graph, both sensors show a gradual decrease in response with increasing relative humidity when tested against a 50ppm target gas, and still have high response values at RH=70%, with Sensor1 having a response of 12.68% for 50ppm ammonia and Sensor3 having a response of 25.46% for 50ppm formaldehyde